

4-43-65-4

STAGNATION POINT FLOW
WITH RADIATION

OCTOBER 1965

TASK IV OF A FUNDED STUDY ON SUPERORBITAL ENTRY
HEATING PROBLEMS UNDER CONTRACT NAS 7-295

PREPARED BY:

R. F. Chisnell / R.F.C.
R. F. Chisnell, Consultant, Reader
University of Manchester

H. Hoshizaki
H. Hoshizaki, Senior Member
Aerospace Sciences Laboratory

L. E. Lasher
L. E. Lasher, Member
Aerospace Sciences Laboratory

FOREWORD

The work described in this report was completed for the National Aeronautics and Space Administration Headquarters, under the terms and specifications of their Contract NAS 7-295, issued through their Western Operations Office, 150 Pico Boulevard, Santa Monica, California - 90406.

This work was performed in Lockheed Missiles and Space Company's Aerospace Sciences Laboratory under R. D. Moffat, Manager.

ACKNOWLEDGEMENTS

The writers would like to express their sincere appreciation to K. H. Wilson and M. J. Rosen of the laboratory for their helpful discussions and suggestions during the course of the work described in this report. Particular thanks are extended to H. R. Kirch and A. E. Dandridge for their contributions in the I.B.M. code programming and development.

ABSTRACT

16 984

The coupling between the inviscid and viscous flows in the hypersonic stagnation region is investigated at high flight velocities where radiative energy transport is significant. A simple analytic solution for the flow field is found, in which the velocity field is expressed in terms of the density and two position coordinates. Solutions to the energy equation were obtained, including radiation transport for a gray gas, using the analytic flow field solution.

The results of the analysis show that under some conditions, the reduction in the convective heating due to radiation cooling can be predicted by an inviscid flow analysis. It is also concluded that second-order boundary-layer effects do not play an important role in radiatively coupled flow fields.

Author

NOMENCIATURE

Subscript s denotes conditions behind the shock on the line of symmetry.

Numerical subscripts refer to the number of the term in the series expansion of the function.

C	$=$	$\rho_{\infty} k_s / \kappa$
$B(\tau)$	$=$	$\frac{1}{\pi} \sigma T_1^4$
\bar{B}	$=$	$B(\tau) / B(\tau_s)$
$E_n(x)$	$=$	$\int_0^1 \mu^{n-2} e^{-x/\mu} d\mu$
h	$=$	specific enthalpy
κ	$=$	body radius of curvature
k_R	$=$	radiation volumetric absorption co-efficient
k	$=$	k_R / ρ
\bar{k}	$=$	k / k_s
Pr	$=$	$c_p \mu / K$
q^R	$=$	radiative flux
Re	$=$	$\rho_{\infty} V / \kappa \mu_s$
u	$=$	velocity component parallel body
v	$=$	velocity component perpendicular body
V	$=$	incident stream velocity
m	$=$	exponent in $\bar{k} = h_1^m$; = 2.1, 4.25
n	$=$	exponent in $h_1 \propto T_1^n$; = 5/3

x = distance along body
y = distance perpendicular body
z = Dorodnitsyn variable
 $\beta = \epsilon \text{ Re Pr}$
 $\Gamma =$ Radiation parameter
 $\epsilon = \rho_{\infty} / \rho_s$
 $\theta =$ body angle
K = heat conduction co-efficient
 $\mu =$ viscosity co-efficient
 $\rho_{\infty} =$ density ahead of shock
 $\tau =$ optical thickness

1. INTRODUCTION

At high flight velocities where radiative energy transport is significant, there exists a coupling between the viscous and inviscid flow regions in the shock layer. This coupling is due to radiation cooling and the transfer of energy by emission and absorption. The purpose of the present investigation is to examine this coupling in detail to determine whether or not the convective heating can be predicted by separating the shock layer flow field into an inviscid and viscous region. When the shock layer gas is assumed to emit but not to absorb radiant energy, the inviscid flow solution will yield a zero wall temperature and thus does not provide a driving potential for the convective heating.¹ When self absorption is taken into account, the inviscid flow solution will yield a finite wall temperature.² In the present investigation, inviscid and viscous solutions are obtained in the region of the stagnation point of a blunt body for a gas that both emits and absorbs radiative energy. The viscous solution yields both the convective and radiative heating to a surface. The inviscid solution yields only the wall enthalpy which, in conjunction with boundary layer theory, can be used to predict the convective heating. More precisely, then, we would like to determine the conditions under which the inviscid flow solution, for an emitting and absorbing gas, can be used with boundary layer theory to predict the convective heating. The complete viscous solution is used as a basis of comparison. A second objective of this investigation is to determine whether or not any discrepancies between the convective heating, obtained by the inviscid flow plus boundary layer solutions, and the convective heating predicted by the complete viscous solution, can be made up by second-order boundary-layer theory.

A new hypersonic stagnation region flow field is used to investigate the coupling between the inviscid and viscous flows. Goulard³ suggested a correspondence between the radiating and non-radiating stagnation flow regimes, which enabled him to solve the energy equation, the only equation where radiative effects are important. In this analysis the hypersonic approximation of small

density ratio, ϵ , across the shock is used. To the lowest order in ϵ , the continuity and momentum equations are found to have a simple analytic solution in the stagnation region, in which the velocity field is expressed in terms of the density and two position co-ordinates, the one normal to the body being Dorodnitsyn. This solution is used in place of the correspondence between radiating and non-radiating flows suggested by Goulard.

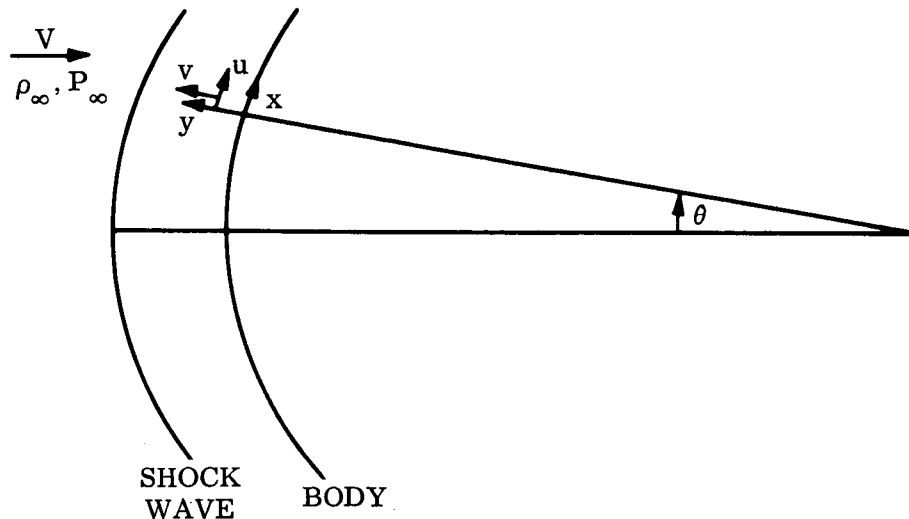
2. HYPERSONIC STAGNATION POINT FLOW

Fig. 1

In this section a simple analytic axi-symmetric hypersonic flow solution, valid in the stagnation region, is obtained. Boundary layer co-ordinates are used, as indicated in Fig. (1). The velocity component, u , parallel to the body surface, $y = 0$, is an odd function of distance, x , along the body surface and all other flow variables are even functions of x . We therefore make the following series expansions:

$$\begin{aligned}
 u/(\kappa x V) &= u_1(y) + (\kappa x)^2 u_2(y) + \dots \\
 v/(\epsilon V) &= v_1(y) + (\kappa x)^2 v_2(y) + \dots \\
 P/\{(1 - \epsilon)\rho_\infty V^2\} &= P_1(y) + (\kappa x)^2 P_2(y) + \dots \\
 \rho/\rho_s &= \rho_1(y) + (\kappa x)^2 \rho_2(y) + \dots
 \end{aligned}
 \tag{1}$$

where ρ_∞ , V , are the density, fluid velocity of the incident stream, κ is the curvative of the axi-symmetric body at the stagnation point, the suffix

s denotes conditions immediately behind the shock along the line of symmetry, $x = 0$, and $\epsilon = \rho_\infty/\rho_s$. The flow variables have been non-dimensionalized with respect to their values just behind the shock on $x = 0$, see Eq. (3). Only the first terms in these expansions are considered in this report; the authors intend to consider the second terms at a later date.

The conservation equations across the shock are;

$$\begin{aligned}\rho_\infty V \cos \theta &= -\rho v \\ V \sin \theta &= u \\ P_\infty + \rho_\infty V^2 \cos^2 \theta &= P + \rho v^2 \\ h_\infty + \frac{1}{2} V^2 \cos^2 \theta &= h + \frac{1}{2} v^2\end{aligned}\tag{2}$$

where h is the specific enthalpy and θ is the angle of inclination of the body normal to the axis of symmetry. For small θ , θ may be taken as κx and Eqs. (2) give

$$u_s = \kappa x V, \quad v_s = -\epsilon V, \quad P_s = \rho_\infty V^2 (1 - \epsilon)\tag{3}$$

neglecting P_∞ in comparison with P_s . These are the values used to non-dimensionalize (1).

The continuity and x-momentum equation for a thin inviscid shock layer are (Hayes and Probstein⁴, p. 388)

$$\begin{aligned}\frac{1}{x} \frac{\partial}{\partial x} (\rho u x) + \frac{\partial}{\partial y} (\rho v) + 2\kappa \rho v &= 0 \\ u \frac{\partial u}{\partial x} + v \frac{\partial u}{\partial y} + \kappa u v &= -\frac{1}{\rho} \frac{\partial P}{\partial x} \\ u \frac{\partial v}{\partial x} + v \frac{\partial v}{\partial y} - \kappa u^2 &= -\frac{1}{\rho} \frac{\partial P}{\partial y}\end{aligned}\tag{4}$$

Substituting (1) into (4) and keeping only the lowest order in x , the equations give

$$2\rho_1 u_1 + \frac{\epsilon}{\kappa} \frac{d}{dy} (\rho_1 v_1) + 2\epsilon \rho_1 v_1 = 0$$

$$u_1^2 + \frac{\epsilon}{\kappa} v_1 \frac{du_1}{dy} + \epsilon u_1 v_1 = \frac{2\epsilon(1-\epsilon)}{\rho_1} \quad (5)$$

$$\epsilon^2 v_1 \frac{dv_1}{dy} = -\frac{\rho_\infty}{\rho_1} (1-\epsilon) \frac{dP_1}{dy}$$

These equations must be solved subject to the boundary conditions

$$u_1 = 1, \quad v_1 = -1, \quad \rho_1 = 1, \quad P_2 = -1, \quad P_1 = 1 \quad (6)$$

at the shock $y = y_s$, and $v_1 = 0$ at the body $y = 0$.

We now utilize the hypersonic approximation of small ϵ . We note first of all that since the shock stand off distance is of order ϵ , that $\frac{1}{\kappa} \frac{d}{dy}$ is of order ϵ^{-1} . Having established the order of magnitude of the $\frac{d}{dy}$ operator, we may now approximate Eqs. (5) for small ϵ . Terms neglected are, at the shock, ϵ times smaller than those retained,

$$2\rho_1 u_1 + \left(\frac{\epsilon}{\kappa} \frac{d}{dy}\right) (\rho_1 v_1) = 0$$

$$u_1^2 + v_1 \left(\frac{\epsilon}{\kappa} \frac{d}{dy}\right) u_1 = 0 \quad (7)$$

The third Eq. of (5) shows that p_1 varies negligibly across the layer. Note that these equations may be written as differential equations for u_1 and $\rho_1 v_1$ and the operator $\frac{\epsilon}{\kappa \rho_1} \frac{d}{dy}$, with no further dependence on the density function ρ_1 . We therefore introduce the Dorodnitsyn independent variable

$$z = \frac{\kappa}{\epsilon} \int_0^y \rho_1 dy \quad (8)$$

and Eqs. (7) become

$$2u_1 + \frac{d}{dz} (\rho_1 v_1) = 0 \tag{9}$$

$$u_1^2 + (\rho_1 v_1) \frac{du_1}{dz} = 0$$

The appropriate boundary conditions are $u_1 = 1$, $\rho_1 v_1 = -1$ at the shock $z = z_s$ and $\rho_1 v_1 = 0$ at $z = 0$. The value of z_s has to be determined in the solution.

The solution is

$$\begin{aligned} u_1 &= z \\ \rho_1 v_1 &= -z^2 \\ z_s &= 1 \end{aligned} \tag{10}$$

This solution will be used in the next section. It is attractive both for its simplicity and its generality, being valid for all density distributions ρ_1 .

The following limitations must be noted. Firstly, only the first terms in an expansion around the body are used. Secondly, these terms are determined only to their first terms in an ϵ expansion. To this order of approximation the shock has been found to be at $z_s = 1$. In the particular case of a constant density solution, Eq. (8) gives a stand-off distance ϵ/κ . This agrees with the first term of the exact constant density solution for a sphere, due to Lighthill⁵, which gives a stand-off distance

$$\frac{\epsilon}{\kappa} \left(1 - \sqrt{\frac{8\epsilon}{3}} + 3\epsilon + \dots \right)$$

for small ϵ , (see Hayes and Probstein p. 159). The solution (10) may be extended by substituting a series expansion in ϵ for the flow variables into (5), the first terms in the series being given by (10). The derivation of the second term is not presented here, but it is encouraging to note that, in the

constant density case, the stand-off distance is given $\frac{\epsilon}{\kappa} \left(1 - \sqrt{\frac{8\epsilon}{3}} \right)$. Thirdly, and finally, we return to the approximations made to Eqs. (5) for small ϵ . The order of magnitudes of the terms were determined from their known values immediately behind the shock. The solution (10) may therefore be used only in a region in which the same orders of magnitude apply. Only the first two terms in the second of Eqs. (5) are retained, and of these the second term tends to zero on the body as $v_1 = 0$ there, forcing both the retained terms to tend to zero at the body. Hence, near the wall, the neglected pressure gradient term will become **larger** than the retained terms, which behave quadratically with z . The pressure term therefore exceeds the retained terms in a sub-layer $\frac{1}{\kappa} \epsilon^{3/2}$ thick. As the sub-layer occupies only $\epsilon^{1/2}$ of the shock layer, only small departures from (10) are caused by neglecting the pressure term.

For the viscous solution, a term $\frac{1}{\rho} \frac{\partial}{\partial y} \left(\mu \frac{\partial u}{\partial y} \right)$ is included in the right hand side of the second of Eqs. (4). We note that if $\mu \alpha \frac{1}{\rho}$ this viscous term is proportional to $\frac{d^2 u_1}{dz^2}$ and hence the solution (10) is still valid.

3. RADIATION IN THE STAGNATION REGION

The work in this section is based upon that of Goulard³ and Thomas². In the stagnation region the kinetic energy is neglected in comparison with the specific enthalpy and viscous dissipation in comparison with heat conduction. The temperature, T , and the enthalpy in the stagnation region will be even functions of x . The last of the shock Eqs. (2) shows that $h_s = 1/2V^2$, neglecting h_∞ and $1/2v^2$. We therefore substitute

$$h/\left(\frac{1}{2}V^2\right) = h_1(y) + (\kappa x)^2 h_2(y) + \dots \quad (11)$$

$$T = T_1(y) + (\kappa x)^2 T_2(y) + \dots$$

in the energy equation and keep only the terms independent of x , giving

$$\left(\frac{1}{2}\rho_s \epsilon V^3\right)\rho_1 v_1 \frac{dh_1}{dy} = \frac{d}{dy} \left(K \frac{dT_1}{dy} \right) - \frac{dq^R}{dy} \quad (12)$$

where K is the co-efficient of thermal conduction and q^R is the radiative flux. For the radiative flux, a one-dimensional formulation is used along with the gray gas approximation (see Goulard³),

$$\frac{dq^R}{dy} = \pi k_R \left[4B(\tau) - 2 \int_0^{\tau_s} B(t) E_1 |t - \tau| dt \right] \quad (13)$$

where k_R is the radiation volumetric absorption co-efficient, B is the Planck function

$$\frac{1}{\pi} \sigma T_1^4, \quad \tau = \int_0^y k_R dy$$

is optical length, τ_s its value at the shock and

$$E_n(x) = \int_0^1 \mu^{n-2} e^{-x/\mu} d\mu$$

Define

$$k = \frac{k_R}{\rho}, \quad Re = \frac{\rho_\infty V}{\kappa \mu_s}, \quad \Gamma = \frac{4\pi B(\tau_s) k_s}{\kappa V h_s} \quad (14)$$

$$\beta = \epsilon Re Pr, \quad Pr = \frac{C_p \mu}{K}$$

where $1/2 V^2 dh_1 = C_p dT_1$ and μ_s is the viscosity behind the shock. Assume that the viscosity varies inversely with density, $\rho \mu = \rho_s \mu_s$ and that Pr is constant. Substitution of $\rho_1 v_1$ from (10) and replacing y by z from (7) there follows

$$\frac{1}{\beta} \frac{d^2 h_1}{dz^2} + z^2 \frac{dh_1}{dz} = \Gamma \bar{k} \left[\bar{B}(\tau) - \frac{1}{2} \int_0^\tau \bar{B}(t) E_1 |t - \tau| dt \right] \quad (15)$$

where $\bar{B}(\tau) = B(\tau)/B(\tau_s)$ and $\bar{k} = k/k_s$. We postulate that nondimensional enthalpy and temperature are related by an n^{th} power law, $h_1 \propto T_1^n$, giving $\bar{B}(\tau) = h_1^{4/n}$ and (15) becomes

$$\frac{1}{\beta} \frac{d^2 h_1}{dz^2} + z^2 \frac{dh_1}{dz} = \Gamma \bar{k} \left[h_1^{4/n} - \frac{1}{2} \int_0^\tau h_1^{4/n} E_1 |t - \tau| dt \right] \quad (16)$$

This equation has to be solved in conjunction with the definition of

$$\tau = \int_0^y k_R dy = \frac{\rho_\infty}{\kappa} \int_0^z k dz$$

or in differential form

$$\frac{d\tau}{dz} = \frac{\rho_\infty k_s}{\kappa} \bar{k} \quad (17)$$

Following Thomas we assume a power law dependence of \bar{k} on h_1 , $\bar{k} = h_1^m$. Thomas actually assumes a power law variation between k_R and T. This is equivalent as the pressure variation across the shock layer is negligible to the lowest order in ϵ .

Rewriting $\frac{dh_1}{d\tau}$, in (16) as $\frac{dh_1}{dz} \frac{dz}{d\tau}$ the equations are a pair of ordinary differential equations for h_1 and τ ,

$$\frac{1}{\beta} \frac{d^2 h_1}{dz^2} + z^2 \frac{dh_1}{dz} = \Gamma h_1^m \left[h_1^{4/n} - \frac{1}{2} \int_0^{\tau_s} h_1^{4/n} E_1 |t - \tau| dt \right] \quad (18)$$

$$\frac{d\tau}{dz} = C h_1^m$$

where

$$C = \frac{\rho_\infty k_s}{\kappa}$$

The boundary conditions are

$$h_1 = 1 @ z = 1$$

$$h_1 = h_B, \tau = 0 @ z = 0 \quad (19)$$

where h_B is the prescribed value of h_1 at the body.

To calculate the radiative heat transfer, we have from (13)

$$q^R = 2\pi \left[\int_0^{\tau} B(t) E_2(\tau - t) dt - \int_{\tau}^{\tau_s} B(t) E_2(t - \tau) dt \right]$$

The total heat radiated from the shock layer is comprised of the contribution at the shock plus the contribution at the body. It is given by:

$$Q_R = \frac{q^R(0) - q^R(\tau_s)}{\rho_\infty V h_s} = \frac{2\pi B(\tau_s)}{\rho_\infty V h_s} \left\{ \int_0^{\tau_s} h_1^{4/n} [E_2(t) + E_2(\tau_s - t)] dt \right\} \quad (20)$$

$$Q_R = \frac{\Gamma}{2C} \left\{ \int_0^{\tau_s} h_1^{4/n} [E_2(t) + E_2(\tau_s - t)] dt \right\}$$

Using the definitions following (14) and Eq. (8) the convective heat transfer can be calculated

$$\left(K \frac{dT}{dy} \right)_{y=0} = \frac{1}{2} V^2 \frac{\kappa}{\epsilon} \left(\frac{dh_1}{dz} \frac{\rho_1 \mu}{Pr} \right)_{z=0} = \frac{1}{2} V^2 \frac{\mu_s \kappa}{\epsilon Pr} \left(\frac{dh_1}{dz} \right)_{z=0}$$

as $\rho\mu$ and Pr are assumed to be constant. Hence, non-dimensionalising,

$$\left(K \frac{dT}{dy} / \frac{1}{2} \rho_\infty V^3 \right)_{y=0} = \left(\frac{1}{\beta} \frac{dh_1}{dz} \right)_{z=0} \quad (21)$$

4. METHOD OF SOLUTION

The viscous equation cf. (18) may be written as follows:

$$\frac{d^2 h_1}{dz^2} + F_1(z) \frac{dh_1}{dz} = F_2(z) \quad (22)$$

where

$$F_1(z) = \beta z^2$$

$$F_2(z) = \beta \Gamma h_1^m \left[h_1^{4/n} - \frac{1}{2} \int_0^{\tau_s} h_1^{4/n} E_1 |t - \tau| dt \right] \quad (23)$$

The formal solution of (22) is given by

$$h_1 = \int_0^z \left\{ \int_0^r \exp \left(- \int_t^r F_1 dt \right) F_2 dt \right\} dr + C_1 \int_0^z \exp \left(- \int_0^r F_1 dr \right) dr + h_B$$

$$C_1 = \frac{1 - h_B - \int_0^1 \left\{ \int_0^r \exp \left(- \int_t^r F_1 dt \right) F_2 dt \right\} dr}{\int_0^1 \exp \left(- \int_0^r F_1 dr \right) dr} \quad (24)$$

Picards' method was used on (24). An initial guess for the $h_1(z)$ profile was tried with the new profile for the iteration procedure being obtained from (24). After several iterations, convergence within 0.001 was attained.

The numerical method used to perform the indicated integrations was found to be inaccurate for large values of F_1 , where β was > 100 . The integral that was the source of the inaccuracies was approximated by an asymptotic expression.

$$\int_0^r F_2 \exp \left(- \int_t^r F_1 dt \right) dt = \int_0^r F_2 \exp \left[- \frac{\beta}{3} (r^3 - t^3) \right] dt \sim F_2(r) \int_0^r \exp [-\beta r^2 (r-t)] dt \quad (25)$$

giving a form that explicitly integrates to

$$\frac{F_2(r)}{\beta r^2} \left(1 - e^{-\beta r^3} \right) \quad (26)$$

One approximation made in obtaining (25) was to expand the argument of the exponential about the point $t = r$ and retain only the first order term in $(r - t)$. The other approximation resulted from the postulation that the main contribution of the integrand occurred at $t = r$. For this reason $F_2(t)$ was set equal to $F_2(r)$.

The asymptotic expression (26) was found to give virtually no error in the integration for $\beta > 100$. For values of $\beta < 100$ the indicated integrations were performed using conventional numerical techniques.

The inviscid equation is given by

$$z^2 \frac{dh_1}{dz} = \Gamma \bar{k} \left[\bar{B}(\tau) - \frac{1}{2} \int_0^\tau \bar{B}(t) E_1 |t - \tau| dt \right] \quad (27)$$

i.e. equation (15) with the term $(1/\beta) d^2 h_1 / dz^2 = 0$.

The boundary condition $h_1 = h_B$ at $z = 0$ is extraneous and is omitted.

To deal with Eq. (27), $\bar{B}(t)$ was expanded about the point $t = \tau$ with only the first two terms in the expansion being retained. The following integrals occur in (27)

$$\int_0^\tau E_1 |t - \tau| dt = 2 - \alpha(\tau)$$

$$\text{where} \quad \alpha(\tau) \equiv E_2(\tau) + E_2(\tau_s - \tau) \quad (28)$$

$$\int_0^\tau (t - \tau) E_1 |t - \tau| dt = \beta_1(\tau)$$

$$\text{where} \quad \beta_1(\tau) \equiv \tau E_2(\tau) - (\tau_s - \tau) E_2(\tau_s - \tau) + E_3(\tau) - E_3(\tau_s - \tau)$$

Using the expansion for $B(t)$, previously stated expressions for $\bar{B}(\tau)$ and \bar{k} , and Eq. (28), Eq. (27) becomes

$$\frac{dh_1}{dz} = \frac{\Gamma \alpha(\tau) h_1^{m+4/n}}{2 \left[z^2 + \frac{2\Gamma}{Cn} \beta_1(\tau) h_1^{-1+4/n} \right]} \quad (29)$$

Formal integration gives

$$h_1 = 1 - \int_z^1 \frac{\Gamma \alpha(\tau) h_1^{m+4/n} dz}{2 \left[z^2 + \frac{2\Gamma}{Cn} \beta_1(\tau) h_1^{-1+4/n} \right]} \quad (30)$$

Picards' method was used on (30) in the same manner that it was used on (24).

In the original formulation of the viscous equation, the handling of $B(t)$ was done in the same manner as that done in the inviscid equation. However, the solutions for large values of β seemed inconsistent using this original formulation. It was felt that using the full expression for $B(t)$ would remedy the inconsistencies and so it was introduced into the viscous equation. It was ascertained later that, in fact, the cause of the inconsistencies was the inaccurate answers that the numerical method of integration provided for $\beta > 100$. However, the full expression for $B(t)$ was retained in the viscous equation. Use of the exact expression for $B(t)$ in the inviscid equation introduces numerical difficulties as the equation is in an indeterminate form at $z = 0$. For this reason the approximate expression was used in the inviscid equation.

A comparison is made between the solutions of the viscous equations with and without the use of the complete expression for $B(t)$ in Fig. 2. This comparison was made to determine the effect of not using the full expression for $B(t)$ in the inviscid equation. It can be seen that the effect on the viscous profile is small, never being over five percent for the example considered. In the results section, this small error is observed in the inviscid solution.

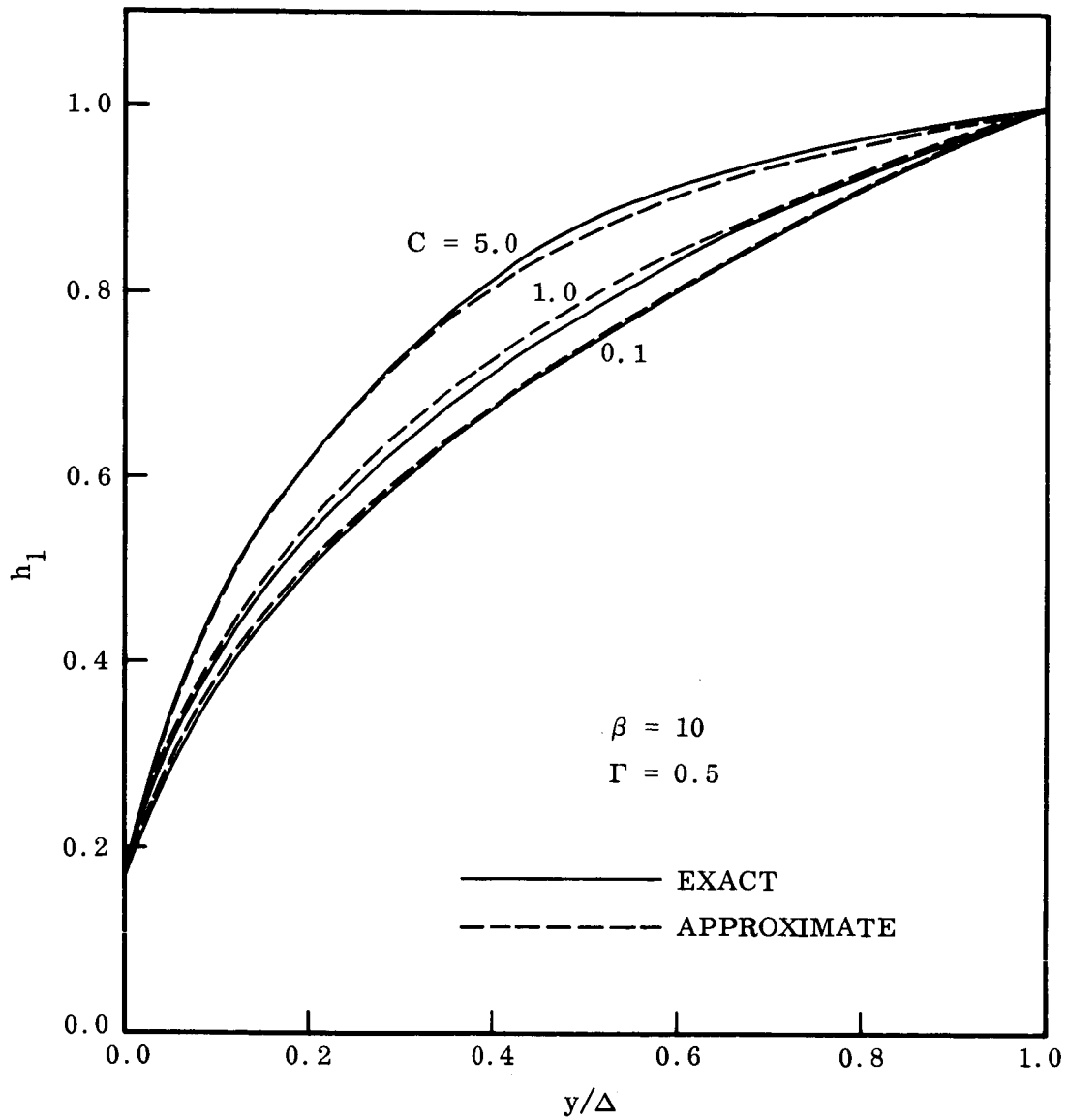


Fig. 2 Viscous Solution With Radiation

5. DISCUSSION OF RESULTS

The solutions to the inviscid and viscous equations were obtained first for typical values of the radiation cooling parameter, Γ , and the Reynolds number parameter, β . The enthalpy profiles for these solutions are presented in Figs. 3 through 5. In Fig. 3 enthalpy profiles for flows without radiation loss are presented for various values of β . It is seen that, as β increases, the viscous region decreases and the enthalpy profile approaches the inviscid enthalpy profile. The point at which the viscous profiles depart from the inviscid profiles is a good indication of the edge of the viscous region.

The effect of increasing the radiation loss parameter for fixed values of the Reynolds number parameter, β , is shown in Figs. 4 and 5. These results show the existence of substantial gradients in the inviscid flow for large values of Γ . Note, however, the pronounced increase in the enthalpy gradients in the viscous layer. The edge of the viscous layer can be easily identified for the zero radiation loss profiles ($\Gamma = 0$).

In order to determine the conditions under which the reduction of the convective heat transfer by radiation cooling can be predicted by considering only the reduction in the driving enthalpy, inviscid and viscous solutions were obtained for fixed flight velocities and a number of free stream altitudes. The pertinent parameters were evaluated for each case and numerical solutions to the appropriate equations were obtained. Viscous solutions with no radiation loss were also obtained to provide a basis of comparison. Typical enthalpy profiles for these cases are presented in Figs. 6 through 9. The slight discrepancy between the inviscid and viscous profiles in the inviscid region of the shock layer is attributed to the different manner employed in evaluating $B(t)$ in the two solutions.

In Fig. 10 ratios of the convective heating with radiation loss to the convective heating without radiation loss, $q_c/(q_c)_0$, are presented as a function of flight altitude. This ratio of the convective heating was obtained from the

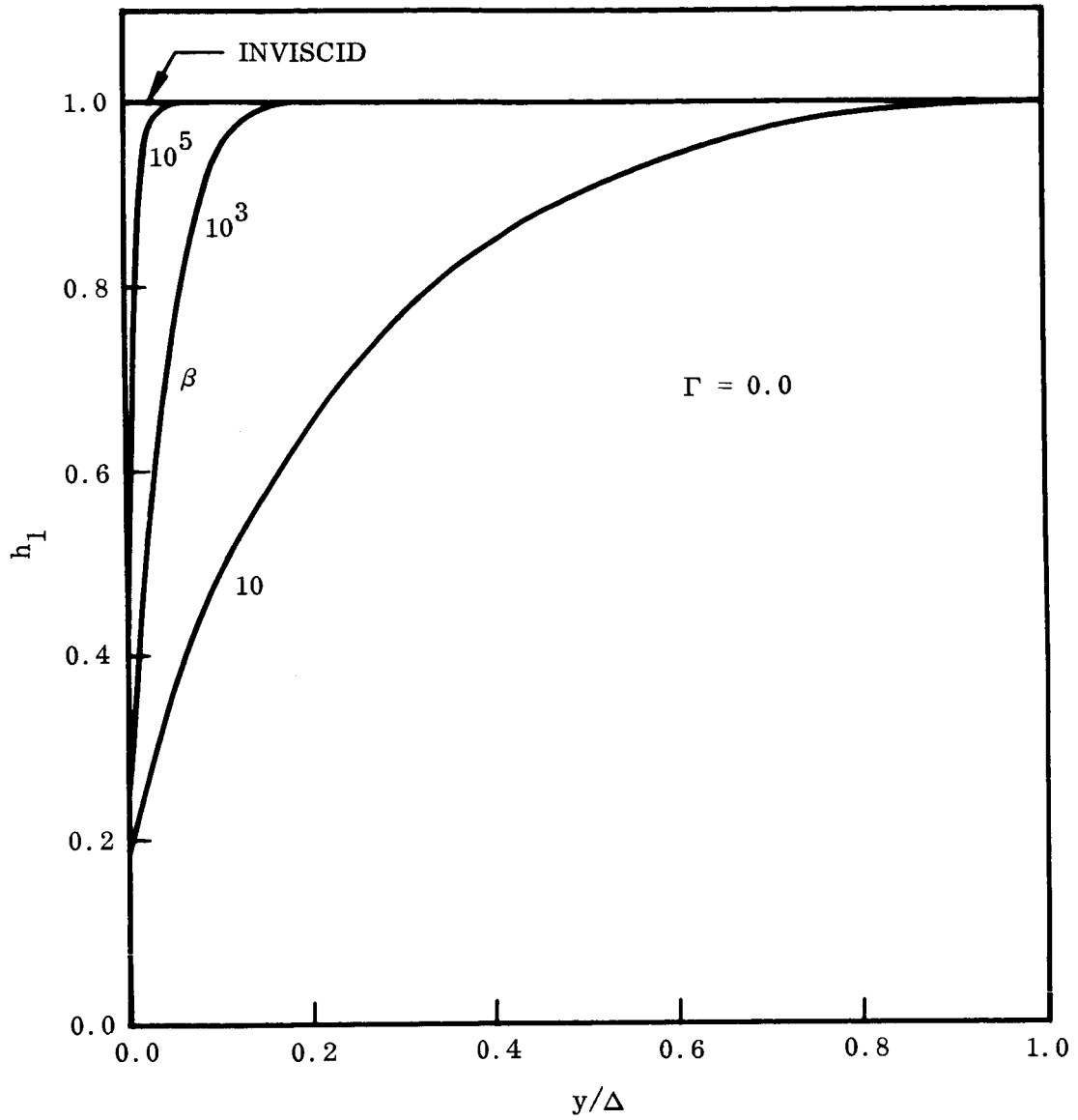


Fig. 3 Inviscid and Viscous Enthalpy Profiles With No Radiation

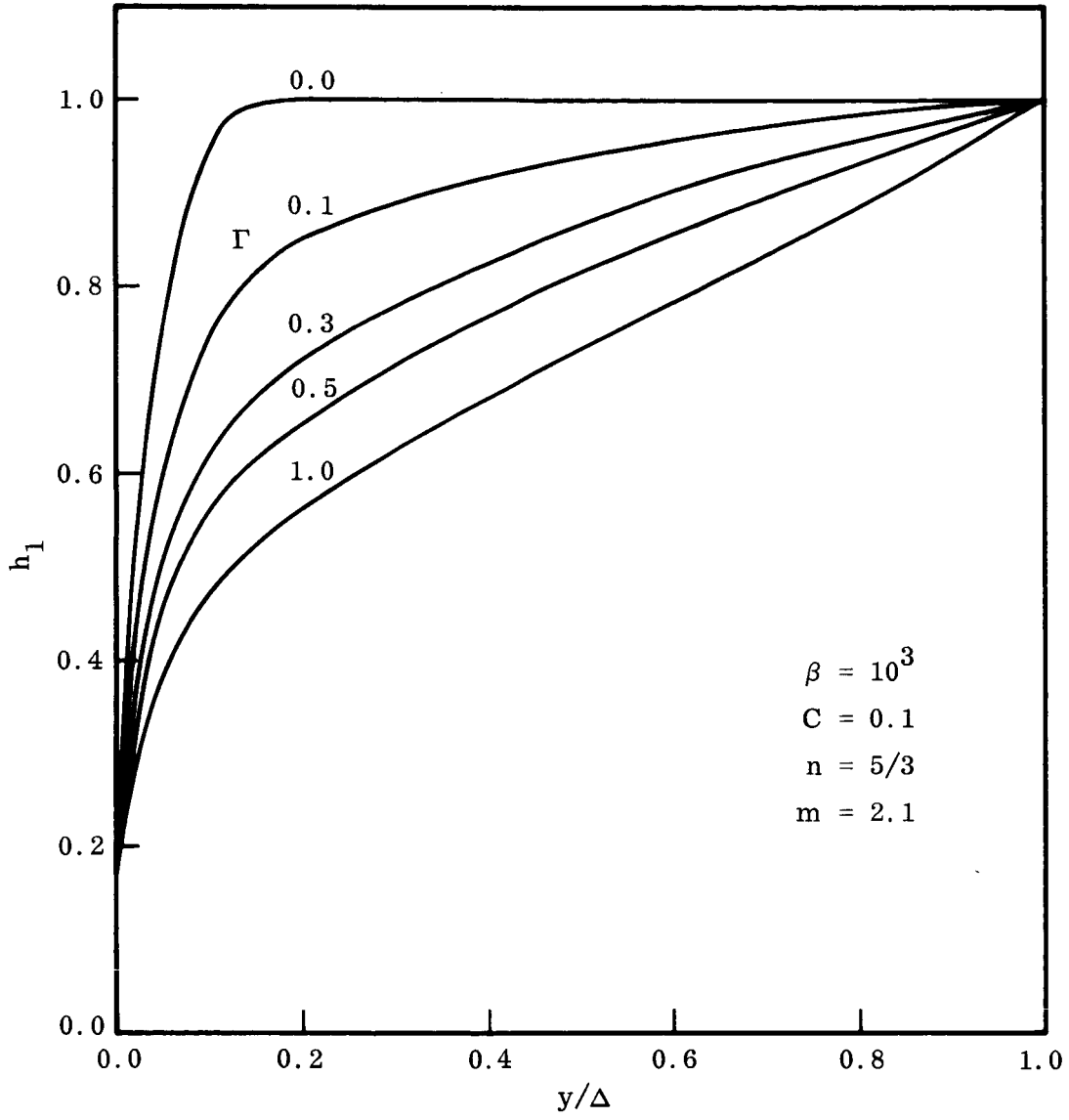


Fig. 4 Viscous Enthalpy Profiles for Different Values of Γ

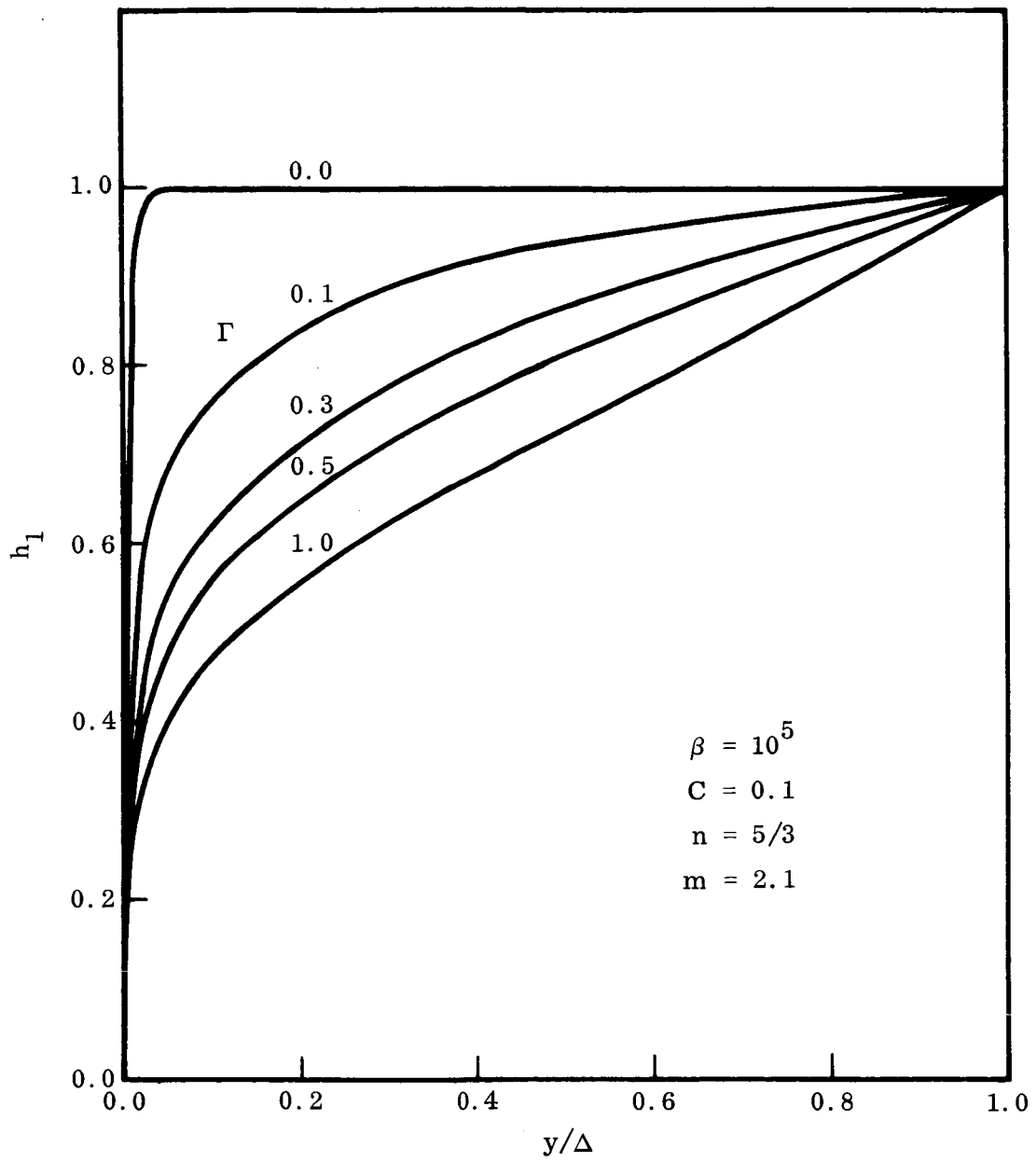


Fig. 5 Viscous Enthalpy Profiles for Different Values of Γ

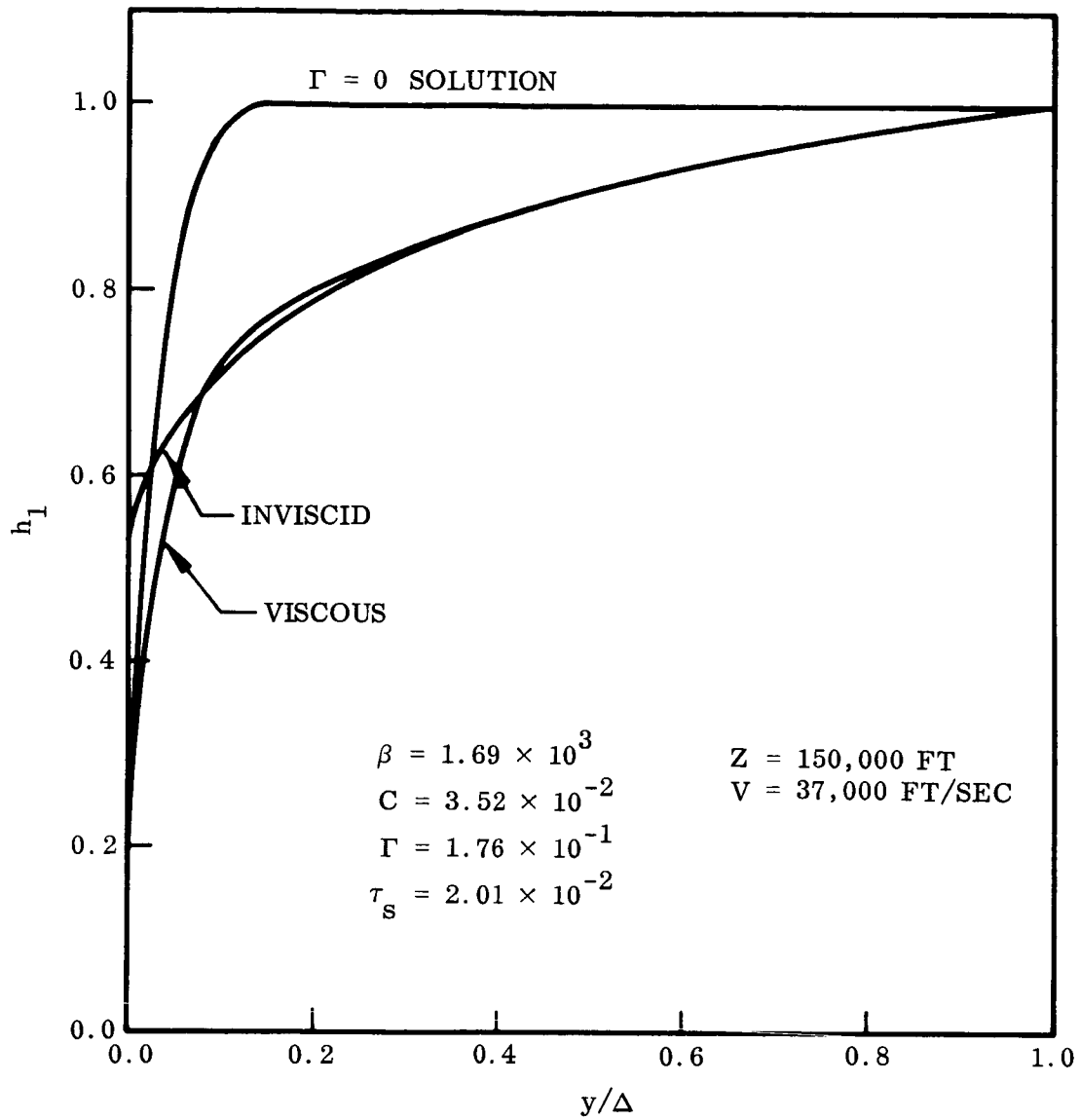


Fig. 6 Viscous and Inviscid Enthalpy Profiles

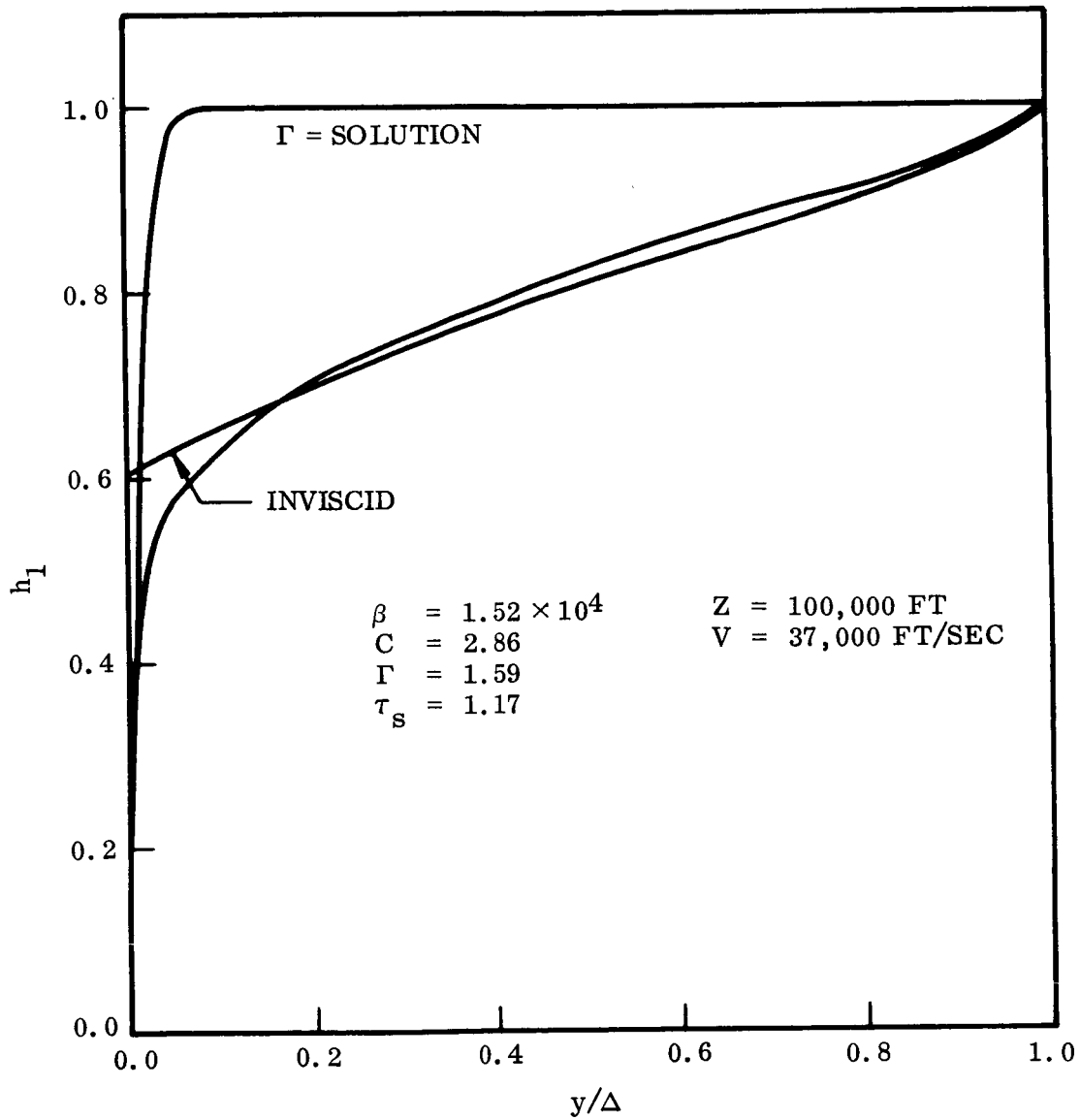


Fig. 7 Inviscid and Viscous Enthalpy Profiles

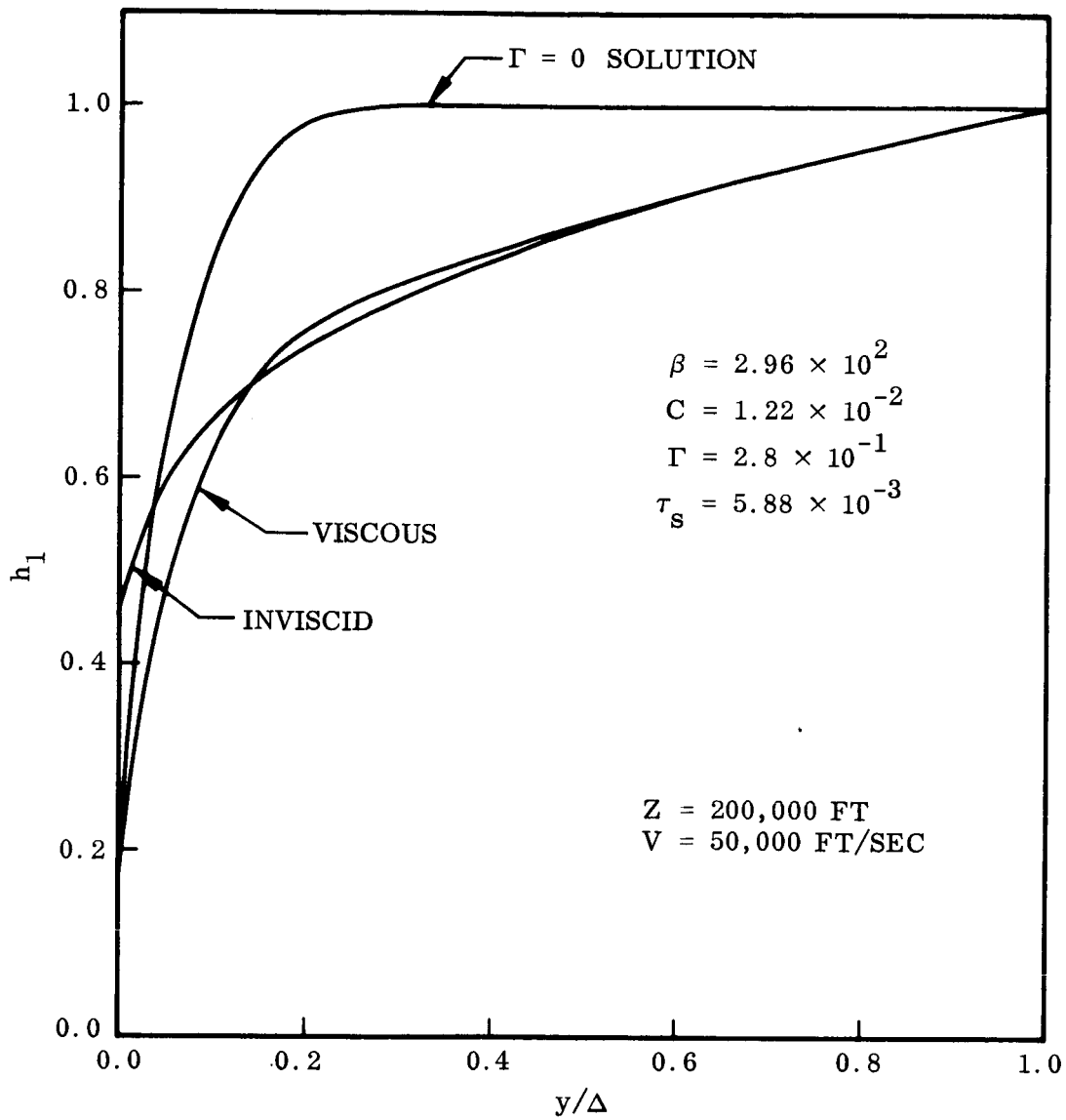


Fig. 8 Viscous and Inviscid Enthalpy Profiles

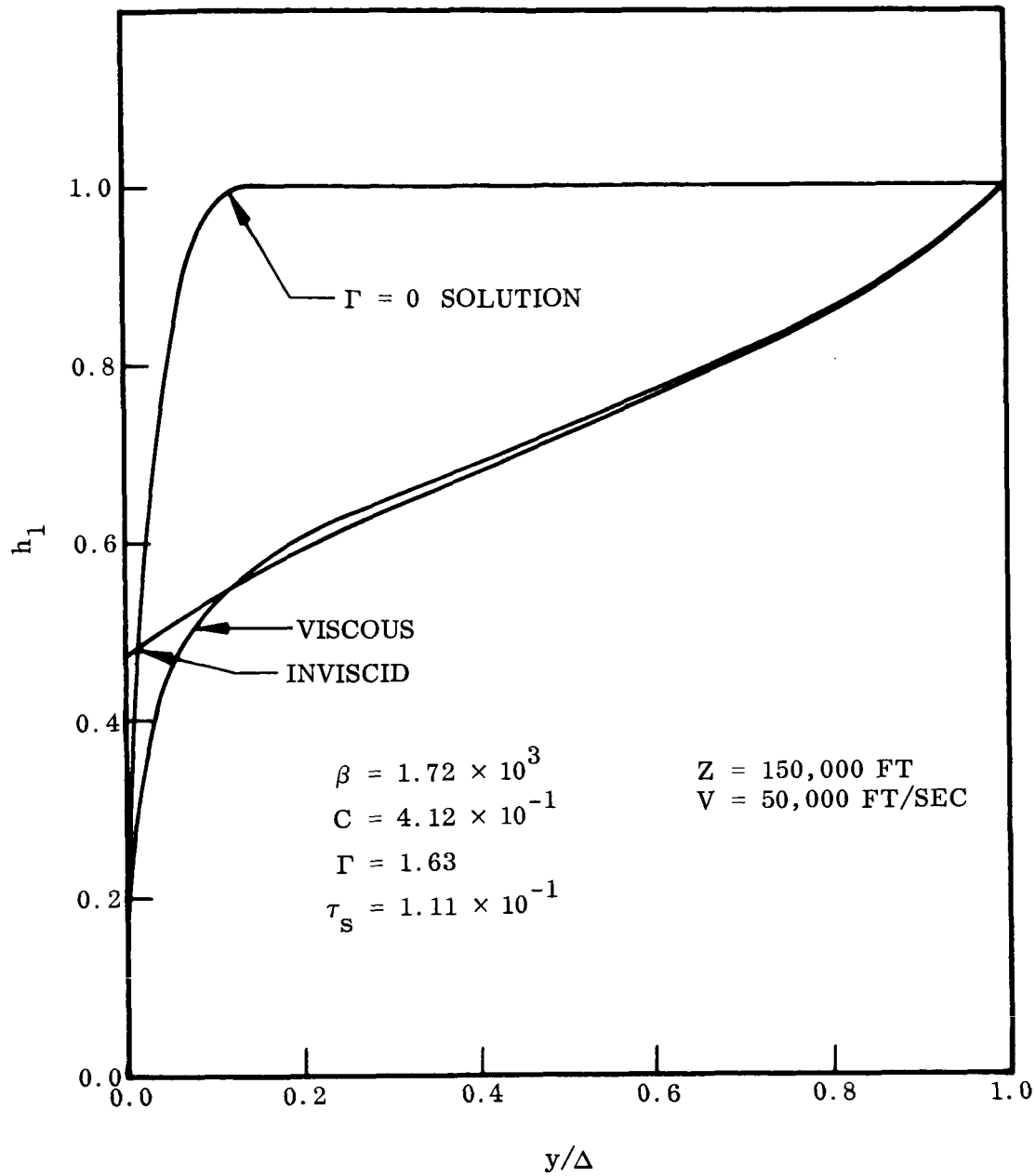


Fig. 9 Viscous and Inviscid Enthalpy Profiles

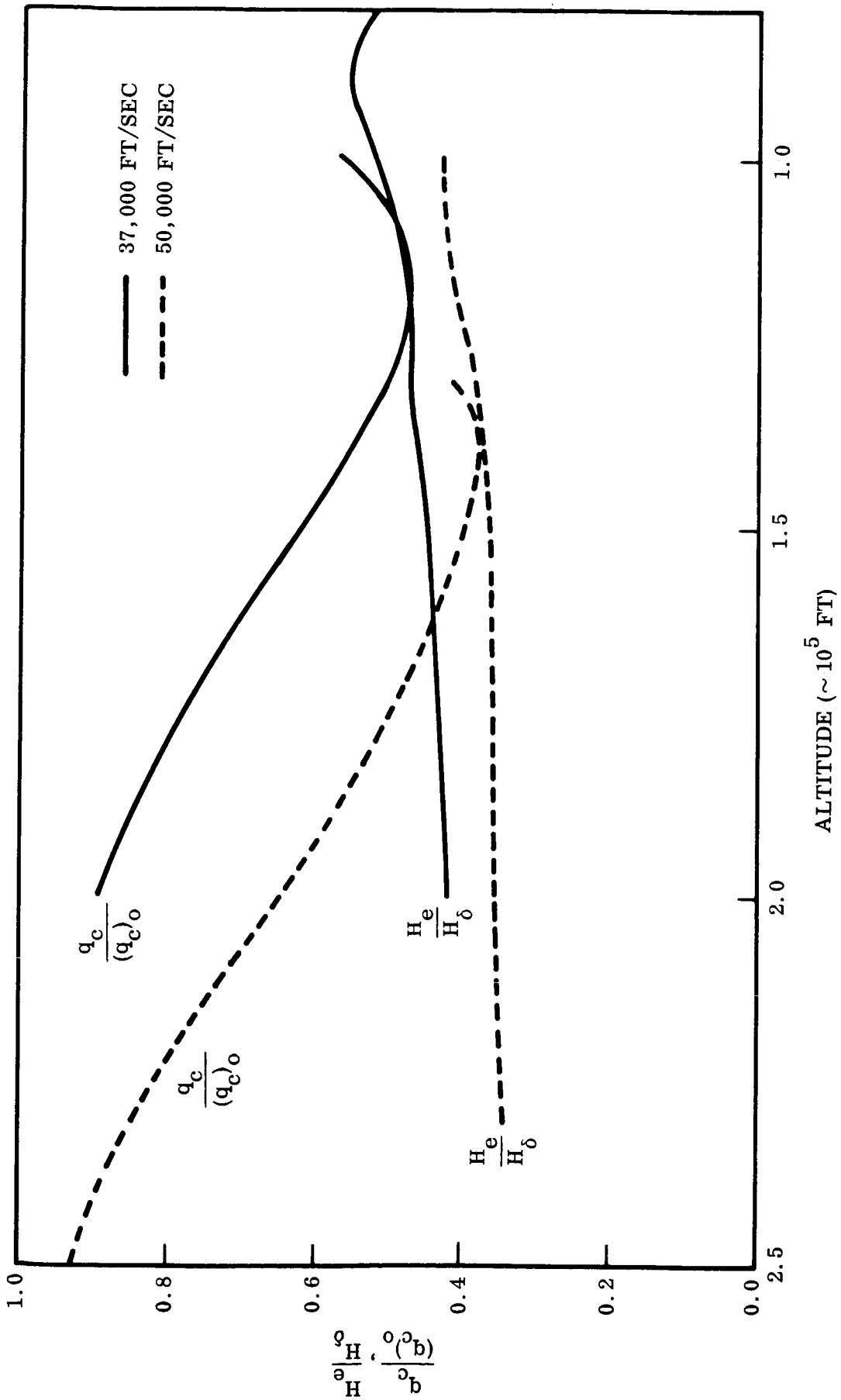


Fig. 10 Convective Heating

viscous solution. Also shown in Fig. 10 are the values of the wall enthalpy as obtained from the inviscid solution for the identical conditions. Since the convective heat transfer can be expressed as

$$q_c = h(H_e - H_w) = K \frac{\partial T}{\partial y}$$

where H_e is the enthalpy obtained from the inviscid solution evaluated at the wall, H_w is the wall enthalpy, and h is the heat transfer coefficient, the reduction in the convective heating by radiation cooling can be accounted for by the reduction in the driving enthalpy, if the heat transfer coefficient is unaffected by radiation cooling. Here we are assuming that in this coupled problem the inviscid flow can be separated from the viscous flow. At high altitudes the shock layer will become optically thin and the radiation loss will be small so that the ratio $q_c/(q_c)_0$ will approach unity and the inviscid wall enthalpy, H_e , will approach zero. As the flight altitude is decreased the inviscid wall enthalpy will increase since the optical depth and absorption of radiant energy increases. On the other hand, decreasing the flight altitude will also increase the radiation loss thereby causing a decrease in the ratio $q_c/(q_c)_0$. At some point where the Reynolds number is sufficiently high the two curves should meet as they appear to do in Fig. 10. For large Reynolds numbers the flow in the shock layer will be primarily inviscid and the radiation cooling processes will be identical in both the viscous and inviscid solutions. Therefore, we would expect that at sufficiently high Reynolds numbers the reduction in the convective heating can be accounted for by the reduction in the wall enthalpy from the inviscid solution. The present results seem to bear this out; however, we were not able to obtain solutions at very low altitudes due to numerical difficulties and the question remains as to what is the correct limiting value for the reduction in the convective heating by radiation cooling.

A second objective of this study was to investigate the possibility that any discrepancy between the reduction in the convective heating as predicted by the viscous analysis and the reduction in the wall enthalpy as obtained from the inviscid solution could be made up by second-order boundary-layer effects. In Appendix A a discussion of second-order boundary-layer theory for the case

where both velocity and enthalpy gradients exist in the external flow is presented. The conclusion reached from a reexamination of the results of Van Dyke is that for the case where the enthalpy varies from one streamline to another but is assumed constant along each streamline, the effect of external enthalpy gradients is not a second-order but a third-order effect. In the actual case, however, the total enthalpy varies along streamlines due to radiation cooling. However, for the cases considered here where the difference between the reduction in the convective heating, $q_c/(q_c)_0$ and the inviscid wall enthalpy, H_e , are of the order of 0.1, the enthalpy gradients in the inviscid flow are quite small and the enthalpy along streamlines varies quite slowly. We therefore conclude that second-order boundary-layer effects cannot make up the difference between the reduction in convective heating, as predicted by a full viscous layer analysis, and the reduction in the driving enthalpy, as predicted by an inviscid shock layer solution.

For nearly optically thin flows a radiation cooled layer will exist in the inviscid flow in which the enthalpy will vary very rapidly along the streamlines. For these situations a second-order boundary-layer theory does not exist. However, the difference between $q_c/(q_c)_0$ and H_e is so large that the effects are not second-order but first-order.

In Fig. 11 and 12 the optical depths at the shock wave for the flight conditions considered in Fig. 10 are presented. We note in passing that the conditions at which the ratio of the convective heating $q_c/(q_c)_0$ approaches the inviscid wall enthalpy H_e is where the optical depth is between 0.1 and 1.0.

The pertinent parameters for the conditions considered in Fig. 11 are tabulated in Tables 1 and 2.

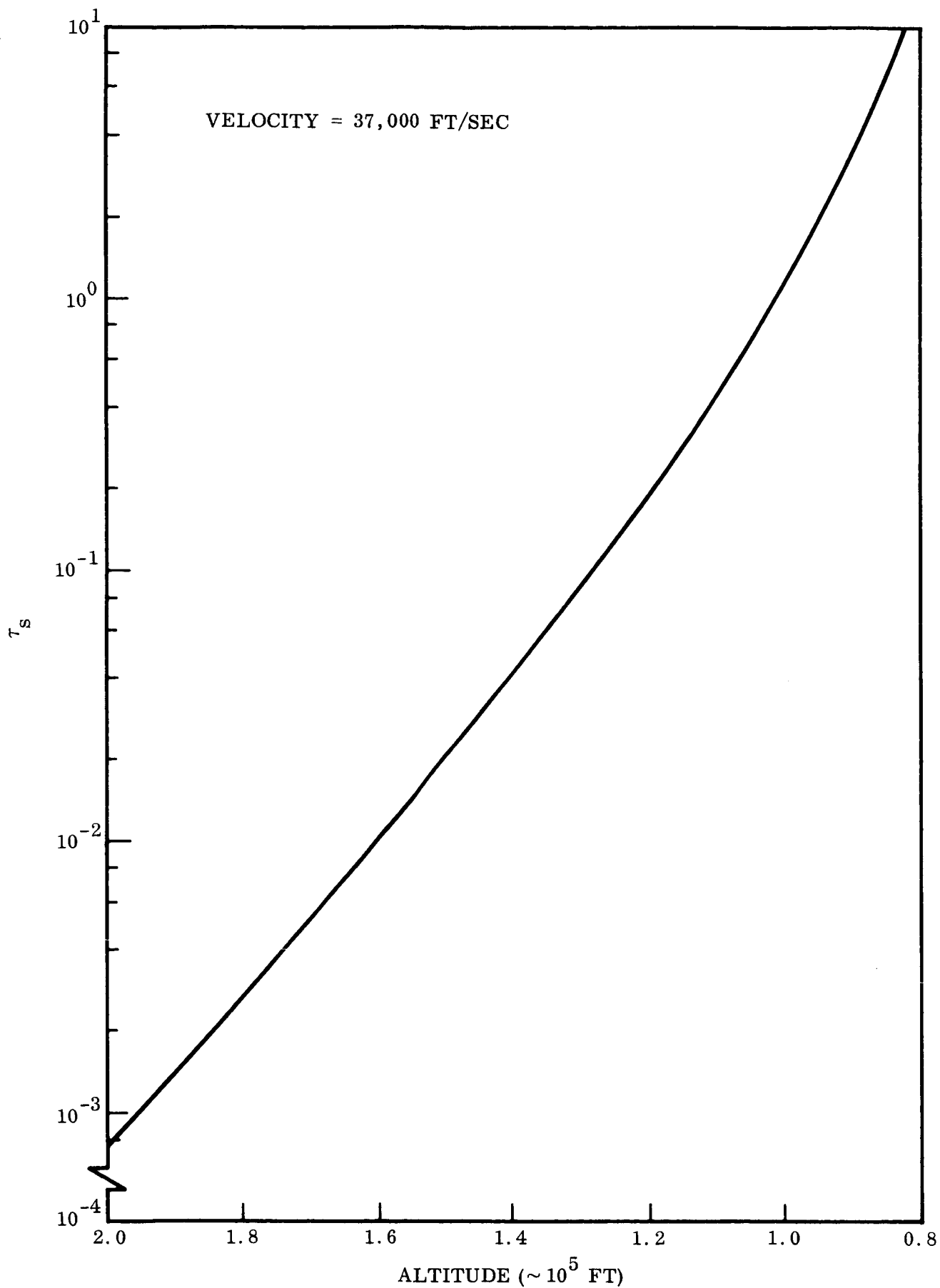


Fig. 11 Optical Depth of the Shock Layer

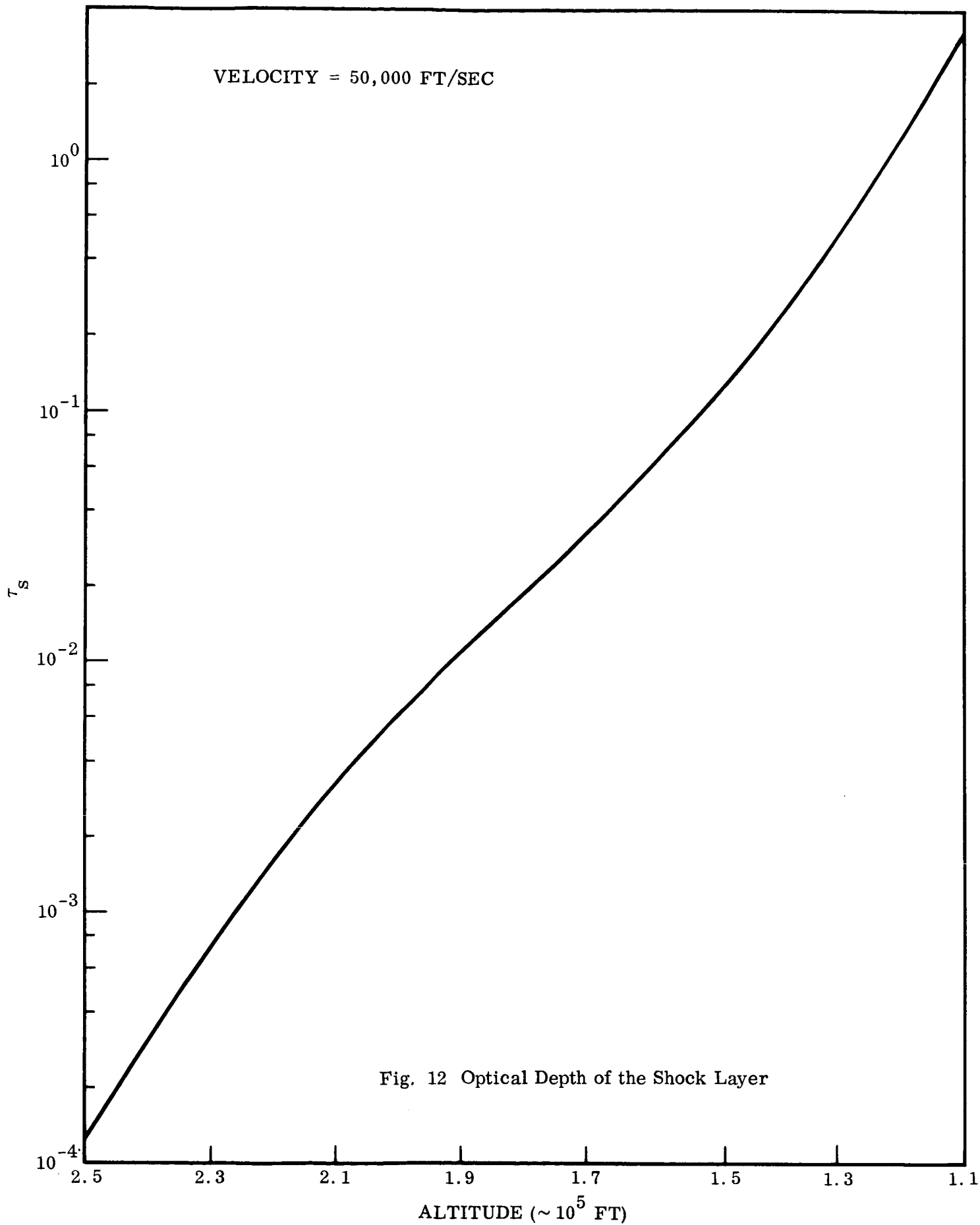


Fig. 12 Optical Depth of the Shock Layer

Table 1
 FLOW FIELD AND FREE STREAM PARAMETERS AT A VELOCITY OF 37,000 ft./sec

Altitude ($\sim 10^3$ ft)	Γ	C	β	$\frac{q_c}{(q_c)_0}$	QR_{visc}	$\tau_{s_{visc}}$	$\frac{\Delta h}{(\Delta h)_0}$	QR_{inv}	$\tau_{s_{inv}}$
200	3.02 E-2	1.04 E-3	2.91 E+2	0.893	2.03 E-2	7.61 E-4	0.417	2.23 E-2	8.42 E-4
180	5.92 E-2	4.00 E-3	5.70 E+2	0.803	3.62 E-2	2.77 E-3	0.430	3.78 E-2	2.93 E-3
150	1.76 E-1	3.52 E-2	1.69 E+3	0.618	7.78 E-2	2.01 E-2	0.448	7.88 E-2	2.05 E-2
130	4.04 E-1	1.86 E-1	3.89 E+3	0.505	1.20 E-1	8.62 E-2	0.472	1.21 E-1	8.82 E-2
120	6.26 E-1	4.47 E-1	6.04 E+3	0.475	1.41 E-1	1.87 E-1	0.474	1.43 E-1	1.92 E-1
110	9.85 E-1	1.11 E+0	9.50 E+3	0.486	1.57 E-1	4.33 E-1	0.492	1.58 E-1	4.45 E-1
100	1.59 E+0	2.86 E+0	1.52 E+4	0.570	1.60 E-1	1.17 E+0	0.523	1.56 E-1	1.17 E+0
90	2.59 E+0	7.65 E+0	2.50 E+4				0.555		
80	4.28 E+0	2.09 E+1	4.13 E+4				0.520	7.60 E-2	1.41 E+1
60	1.12 E+1	1.42 E+2	1.07 E+5				0.415	3.96 E-2	1.16 E+2

Note: $E \pm n \equiv 10^{\pm n}$

Table 2
 FLOW FIELD AND FREE STREAM PARAMETERS AT A VELOCITY OF 50,000 ft/sec

Altitude ($\sim 10^3$ ft)	Γ	C	β	$\frac{q_c}{(q_c)_0}$	QR_{visc}	$\tau_{s_{visc}}$	$\frac{\Delta h}{(\Delta h)_0}$	QR_{inv}	$\tau_{s_{inv}}$
250	3.54 E-2	1.96 E-4	3.75 E+1	0.928	1.83 E-2	1.25 E-4			
230	8.73 E-2	1.19 E-3	9.25 E+1	0.842	4.51 E-2	7.08 E-4	0.340	5.05 E-2	8.06 E-4
200	2.80 E-1	1.22 E-2	2.96 E+2	0.641	1.04 E-1	5.88 E-3	0.353	1.06 E-1	6.14 E-3
180	5.49 E-1	4.71 E-2	5.96 E+2	0.524	1.48 E-1	1.86 E-2	0.356	1.50 E-1	1.90 E-2
150	1.63 E+0	4.12 E-1	1.72 E+3	0.399	2.26 E-1	1.11 E-1	0.362	2.27 E-1	1.14 E-1
140	2.45 E+0	9.41 E-1	2.60 E+3	0.388	2.50 E-1	2.26 E-1	0.368	2.48 E-1	2.29 E-1
130	3.74 E+0	2.18 E+0	3.96 E+3	0.419	2.68 E-1	4.90 E-1	0.382	2.57 E-1	4.84 E-1
120	5.80 E+0	5.25 E+0	6.14 E+3				0.405		
100	1.47 E+1	3.36 E+1	1.55 E+4				0.427	1.41 E-1	1.56 E+1

Note: $E \pm n \equiv 10^{\pm n}$

6. CONCLUSION

Stagnation point flow with radiation was analyzed with the aim being to predict the reduction in the convective heating in a simpler way than using a full viscous analysis. There was discovered a range of velocity-altitude conditions where the reduction in the wall enthalpy, as obtained from the inviscid solution, approximates the reduction in convective heating to the surface. This occurred when the optical depth of the shock layer was between 0.1 and 1.0. The conclusion was also reached that existing second-order boundary-layer effects cannot make up the difference between the reduction in convective heating, as predicted by a full viscous layer analysis, and the reduction in the driving enthalpy, as predicted by an inviscid shock layer solution.

APPENDIX A

THE EFFECT OF ADIABATIC EXTERNAL FLOW GRADIENTS
ON HEAT TRANSFER AT AN AXISYMMETRIC STAGNATION POINT

by M. Van Dyke

In classical boundary-layer theory the boundary layer is regarded as vanishingly thin, so that finite gradients in the external inviscid flow are altogether negligible. The effect of such gradients appears in second-order boundary-layer theory, together with the effects of surface curvature, slip and temperature jump, and boundary-layer displacement. All these second-order effects were analyzed for an axisymmetric stagnation point in reference 6. However, the numerical calculations were limited to an isoenergetic external flow -- one in which the stagnation enthalpy has the same value on every streamline outside the boundary layer. The same is true of the additional computations given in references 7 and 8 for other viscosity laws and surface temperatures.

Fortunately, these results can be reinterpreted to apply to the more general situation in which the external flow is adiabatic but not necessarily isoenergetic -- that is, the stagnation enthalpy, like the entropy, is constant along any one streamline, but may vary from one streamline to another. The results are particularly simple when expressed in terms of the external vorticity. We give here the specific result for a thermally and calorically perfect gas with Prandtl number 0.7 and viscosity proportional to temperature, at the stagnation point of an axisymmetric body that is cooled to 1/5 of the stagnation temperature. The heat transfer is increased from its classical value due to the effects of external gradients by the factor

$$1 + 0.341 \sqrt{\nu_{ST}} \frac{(-\omega/r)_{ST}}{(u/r)_{ST}^{3/2}} \quad (1-A)$$

Here ν is the kinematic viscosity, ω the vorticity, u the velocity parallel to the body, and r the radius from the axis (or distance along the surface); and the subscript ST denotes the limit as the stagnation point is approached in the external inviscid flow. The external vorticity is normally negative, and is conveniently found from

$$\left(-\frac{\omega}{r}\right)_{ST} = \left(\frac{\partial u}{\partial y} \frac{1}{r}\right)_{ST} + \left(\kappa \frac{u}{r}\right)_{ST} \quad (2-A)$$

Here y is the distance normal to the surface of the body, and κ is the curvature (counted positive for a convex body). However, the second-order effects of curvature are often negligible compared with those of external gradients, and then it is consistent to neglect the second term in equation (2-A) compared with the first.

In general, the second-order correction to heat transfer would also contain a term proportional to the gradient of stagnation enthalpy across streamlines. However, this term is absent from equation (1-A) because the effect disappears at a stagnation point; the reason being that the normal to the surface cuts no streamlines.* As we move back on the body, the normal begins to cut streamlines; and the effect is found to grow like the square of the distance from the stagnation point. It would therefore appear in the second term of a Blasius series in which equation (1-A) is the first term.

The form of equation (1-A) holds, with a somewhat different numerical coefficient, for other viscosity laws, values of Prandtl number, and surface temperatures. For Prandtl number still 0.7, but viscosity proportional to the square root of temperature, the values for a wide range of surface temperature can be extracted from references 7 and 8. For incompressible flow, the coefficient in equation (1-A) was found in reference 9 to be 0.5751 for a Prandtl number of 0.7 and 0.5520 for a Prandtl number of unity.

*In incompressible flow, for example, it was found in reference 9 that the second-order heat transfer depends on the inviscid surface gradient of stagnation enthalpy at a cusped plane leading edge (e.g., a flat plate) but not at a blunt one.

The result is accurate when the second-order correction represented by the second term in equation (1-A) is small compared with unity. The result will be only qualitatively correct when both terms are of the same order, and worthless when the second term is large.

For studying flows with thermal radiation, it would be desirable to relax the condition that the external flow is adiabatic. In particular, one would admit a normal gradient of stagnation enthalpy -- and hence of temperature -- at the stagnation point. However, this cannot be done using the equations of reference 6, because in the outer fringes of the boundary layer they describe adiabatic motion, and therefore possess no solutions that will match an external temperature gradient near the stagnation point. Radiative transfer would have to be included in the energy equation for the boundary layer in order to calculate this additional correction to the above result. Although this would seem to be a valuable extension of the theory, it would require considerable analysis.

REFERENCES

1. Hoshizaki, H., and Wilson, K. H., "The Viscous, Radiating Shock Layer About a Blunt Body", AIAA Journal, Vol. 3, No. 9, pp. 1614-1622, September 1965.
2. Thomas, P. D., "On the Transparency Assumption in Hypersonic Radiative Gas Dynamics", AIAA Journal, Vol. 3, No. 8, pp. 1401-1407, August 1965.
3. Goulard, R., "Preliminary Estimates of Radiative Transfer Effects on Detached Shock Layers", AIAA Journal, Vol. 2, pp. 494-503, 1964.
4. Hayes, W. D., and Probstein, R. F., "Hypersonic Flow Theory", Academic Press, 1959.
5. Lighthill, M. J., "Dynamics of a Dissociating Gas, Part I, Equilibrium Flow", Journal of Fluid Mechanics, Vol. 2, pp. 1-32, 1957.
6. Van Dyke, Milton, "Second-Order Compressible Boundary-Layer Theory with Application to Blunt Bodies in Hypersonic Flow", Stanford Univ., Dept of Aero. Engg., SUDAER Rept. No. 112, July 1961; AFOSR-TN-61-1270.
Published under the same title in Hypersonic Flow Research (F. R. Riddell, ed.), Academic Press, New York, 1962, pp. 37-76. However, because no proofs were provided the authors, this version suffers from serious typographical errors and omissions in equations.
7. Davis, R. T. & Flugge-Lotz, I., "Laminar Compressible Flow Past Axisymmetric Blunt Bodies" (Results of a Second-Order Theory). Stanford Univ., Div. of Engg. Mech., Tech. Rept. No. 143, Dec. 1963.
8. Davis, R. T. & Flugge-Lotz, I., "The Laminar Compressible Boundary-Layer in the Stagnation-Point Region of an Axisymmetric Blunt Body Including the Second-Order Effect of Vorticity Interaction", Int. J. Heat & Mass Transfer 7 (1964), pp. 341-370.
9. Van Dyke, Milton, "Higher Approximations in Boundary-Layer Theory", Part 2. Application to Leading Edges, J. Fluid Mech. 14 (1962), pp. 481-495.